HHS Public Access

Author manuscript

J Biol Rhythms. Author manuscript; available in PMC 2022 June 15.

Published in final edited form as:

J Biol Rhythms. 2020 June ; 35(3): 257–274. doi:10.1177/0748730420913205.

The Paralogous Krüppel-like Factors 9 and 13 Regulate the Mammalian Cellular Circadian Clock Output Gene *Dbp*

Joseph R. Knoedler[*,1],

José Ávila-Mendoza[†],

Arasakumar Subramani[†],

Robert J. Denver[*,†,2]

[*]Neuroscience Graduate Program, The University of Michigan, Ann Arbor, Michigan

[†]Department of Molecular, Cellular and Developmental Biology, The University of Michigan, Ann Arbor, Michigan

Abstract

An intricate transcription-translation feedback loop (TTFL) governs cellular circadian rhythms in mammals. Here, we report that the zinc finger transcription factor Krüppel-like factor 9 (KLF9) is regulated by this TTFL, it associates in chromatin at the core circadian clock and clock-output genes, and it acts to modulate transcription of the clock-output gene *Dbp*. Our earlier genome-wide analysis of the mouse hippocampus-derived cell line HT22 showed that KLF9 associates in chromatin with *Per1*, *Per3*, *Dbp*, *Tef*, *Bhlhe40*, *Bhlhe41*, *Nr1d1*, and *Nr1d2*. Of the 3514 KLF9 peaks identified in HT22 cells, 1028 contain E-box sequences to which the transcriptional activators CLOCK and BMAL1 may bind, a frequency significantly greater than expected by chance. *Klf9* mRNA showed circadian oscillation in synchronized HT22 cells, mouse hippocampus, and liver. At the clock-output gene *Dbp*, KLF9 exhibited circadian rhythmicity in its association in chromatin in HT22 cells and hippocampus. Forced expression of KLF9 in HT22 cells repressed basal *Dbp* transcription and strongly inhibited CLOCK+BMAL1-dependent transcriptional activation of a transfected *Dbp* reporter. Mutational analysis showed that this action of KLF9 depended on 2 intact KLF9-binding motifs within the *Dbp* locus that are in close proximity to E-boxes. Knockout of *Klf9* or the paralogous gene *Klf13* using CRISPR/Cas9 genome editing in HT22 cells had no effect on *Dbp* expression, but combined knockout of both genes strongly impaired circadian *Dbp* mRNA oscillation. Like KLF9, KLF13 also showed association in chromatin with clock- and clock-output genes, and forced expression of KLF13 inhibited the actions of CLOCK+BMAL1 on *Dbp* transcription. Our results suggest novel and partly overlapping roles for KLF9 and KLF13 in modulating cellular circadian clock output by a mechanism involving direct interaction with the core TTFL.

[2]To whom all correspondence should be addressed: Robert J. Denver, Department of Molecular, Cellular and Developmental Biology, The University of Michigan, 3264 Biological Sciences Bldg, 1105 N University Ave, Ann Arbor, MI 48109-1085, USA; rdenver@umich.edu.

[1]Present address: Department of Psychiatry and Behavioral Sciences, Stanford University, Stanford, CA 94305.

CONFLICT OF INTEREST STATEMENT

The authors have no potential conflicts of interest with respect to the research, authorship, and/or publication of this article.

Supplemental material is available for this article.

Keywords

circadian clock; transcription; glucocorticoid; Krüppel-like factor; Dbp; clock output

Cellular circadian rhythms in mammals are maintained in part by a cell-autonomous circadian clock consisting of a complex transcription-translation feedback loop (TTFL). At the core of the TTFL are the basic helix-loop–helix-PAS transcription factors Circadian Locomotor Output Cycles Kaput (CLOCK) and aryl hydrocarbon receptor nuclear translocator-like protein 1, also known as BMAL1 (the "positive limb"). CLOCK and BMAL1 heterodimerize and bind to E-box motifs (CACGTG) in the genome, where they activate the transcription of hundreds of genes, including *Period* (*Per*) and *Cryptochrome* (*Cry*) (Dardente and Cermakian, 2007). Their protein products, PER and CRY (the "negative limb"), respectively, then accumulate in the cytoplasm, form PER+CRY heterodimers and translocate to the nucleus, where they disrupt the CLOCK+BMAL1 heterodimer to inhibit transcription of their own genes (Griffin et al., 1999). This leads to a reduction in *Per* and *Cry* mRNAs and protein levels, which in turn leads to a reduction in their ability to disrupt CLOCK+BMAL1. This results in a reciprocal oscillation in the activity of these 2 complexes that takes about 24 h. The CLOCK+BMAL1 heterodimer also binds to E-boxes in the promoters of the orphan nuclear receptor genes *Nr1d1/2* (aka *Rev-erb*α/β) and *Nr1f1* (aka *Ror*α) and regulates daily oscillations in their transcription. Their protein products then regulate the *Bmal1* gene through competitive binding to a retinoid orphan response element in its promoter (Preitner et al., 2002; Ueda et al., 2002; Sato et al., 2004; Abramowitz et al., 2007). This accessory loop regulates the period length of the TTFL. An additional feedback mechanism involves CLOCK+BMAL1 transactivation of *Bhlhe40* and *Bhlhe41* (aka *Dec1* and *Dec2*). These transcription factors repress the transcription from E-box–containing promoters and can inhibit CLOCK+BMAL1 induction of circadian clock- and clock-output genes (Honma et al., 1998; Kawamoto et al., 2004; Nakashima et al., 2008). The kinases CSNK1δ/ε (*Csnk1d* and *Csnk1e*) also regulate the pace of the circadian clock by phosphorylating PER1, which inhibits its nuclear translocation (Vielhaber et al., 2000; Etchegaray et al., 2009). The oscillation in the different components of this loop leads to circadian variation in transcription of circadian clock-output transcription factor genes such as *Dbp*, *Tef*, and *Hlf* (and hundreds of other genes), which in turn mediate circadian variation in physiology, metabolism, oxidative signaling, and other biological processes (Gachon et al., 2006; Dardente and Cermakian, 2007).

While virtually all mammalian cells have circadian oscillators, the master circadian pacemaker is located in the suprachiasmatic nucleus (SCN) of the hypothalamus, which is required for the maintenance of free-running circadian rhythms (Stephan and Zucker, 1972). Projections from the SCN modulate circadian activity of the hypothalamo-pituitary-adrenal axis, resulting in a circadian rhythm in glucocorticoid secretion by the adrenal gland, with peak secretion occurring near the onset of the activity phase (early morning in diurnal mammals, early evening in nocturnal mammals; Dickmeis et al., 2013; Leliavski et al., 2015). Circulating glucocorticoids may act as an entrainment signal for peripheral circadian clocks. For example, adrenalectomy causes phase-shifting of circadian rhythms in peripheral organs, supporting that normal daily oscillations in plasma (glucocorticoid)

maintain synchrony of peripheral clocks with the SCN (Pezuk et al., 2012; Woodruff et al., 2016). Treatment with the synthetic glucocorticoid dexamethasone synchronized circadian rhythms in tissue culture cells and caused temporary phase shifting of circadian rhythms of gene transcription in vivo (Balsalobre et al., 2000). Acute stress and GC treatment caused rapid induction of *Per1* via a glucocorticoid response element (GRE) located in its 5′ flanking region, which may be a mechanism by which glucocorticoids synchronize circadian gene transcription of peripheral clocks (Yamamoto et al., 2005; Reddy et al., 2012).

Krüppel-like factor 9 (KLF9) is a hormone-regulated, zinc-finger transcription factor with diverse functions in development and physiology (Denver, 1999; Cayrou et al., 2002; Bagamasbad et al., 2008; Avci et al., 2012; Mannava et al., 2012; Zucker et al., 2014). We recently conducted a genome-wide analysis of KLF9-regulated genes in the adult mouse hippocampus-derived cell line HT22, which showed that KLF9 primarily associates in chromatin within core promoters and functions predominantly as a transcriptional repressor (Knoedler et al., 2017). Subsequent analysis of our data sets found that many TTFL genes are genomic targets of KLF9. Work from other groups supports that *Klf9* and several other *Klfs*, including the paralogous gene *Klf13*, are clock-output genes (regulated in a circadian manner by the CLOCK+BMAL1 complex; Jeyaraj et al., 2012a; Jeyaraj et al., 2012b; Sporl et al., 2012; Yoshitane et al., 2014; Han et al., 2015). In addition to its regulation by the circadian TTFL, *Klf9* is strongly induced by glucocorticoids (e.g., cortisol, corticosterone), acting via the glucocorticoid receptor (GR) at 2 evolutionarily conserved GREs located 5 to 6 kb upstream of the transcription start site (TSS; Bagamasbad et al., 2012). The paralogous gene *Klf13* is also directly regulated by liganded GR via a GRE located in the intron (Cruz-Topete et al., 2016; Bagamasbad et al., 2019). Sporl and colleagues (2012) showed that circadian variation in *Klf9* mRNA levels in human keratinocytes was correlated with changes in plasma cortisol concentration, and KLF9 acted downstream of the circadian TTFL to affect circadian variation in keratinocyte proliferation. However, to our knowledge, no studies have implicated KLF9 or other KLFs in the regulation of transcription of core clock or clock-output genes.

In the current study, we first focused on potential roles for KLF9 in the regulation of circadian clock and clock-output genes. We looked at circadian changes in *Klf9* mRNA and KLF9 association in chromatin at TTFL genes in mammalian neuronal cells. We tested whether KLF9 can directly regulate transcription of the clock-output gene *Dbp*. We also investigated whether KLF13, which is paralogous to KLF9, can regulate circadian clock genes and might compensate for the loss of KLF9 and vice versa. Our findings support that KLF9 and KLF13 directly regulate the clock output gene *Dbp* and have the potential to influence the transcription of other TTFL genes.

MATERIALS AND METHODS

Bioinformatics Analysis

We analyzed data from our previously published study (Knoedler et al., 2017) in which we conducted chromatin-streptavidin precipitation followed by deep-sequencing (ChSP-seq) to identify KLF9 genomic targets in the mouse hippocampus-derived cell line HT22. Using HOMER (Heinz et al., 2010), we identified enriched E-box motifs within KLF9 ChSP-

seq peaks and mapped their proximity to KLF9 consensus motifs. We used GeneCoDis (Carmona-Saez et al., 2007; Nogales-Cadenas et al., 2009; Tabas-Madrid et al., 2012) for gene ontology analysis on genes with KLF9 peaks. We visualized the locations of CLOCK chromatin immunoprecipitation (ChIP)-seq peaks identified by Yoshitane and colleagues (Raney et al., 2014; Yoshitane et al., 2014) in mouse liver using the UCSC genome browser. We used the UCSC genome browser's sequence conservation track to align and download mammalian *Dbp* intronic sequences to evaluate evolutionary conservation of E-box and GC-box motifs (Kent et al., 2002).

Animal Care and Use

We purchased C57BL/6 mice from the Jackson Laboratory (Bar Harbor, ME) and reared them on a 12L:12D photoperiod with food and water provided ad libitum. To analyze daily variation in gene expression and KLF9 recruitment to chromatin, we housed 6- to 8-month-old male mice in a four-chamber lightproof cabinet with separate light timers to minimize disturbance prior to tissue collection. We then killed mice by rapid decapitation at 4-h intervals beginning at zeitgeber time 2 (ZT02; 2 h after lights-on) for 20 h (final collection point was at ZT22, or 2 h before lights-on; $n = 4$ animals/time point). We dissected the brain to isolate the hippocampal region, collected liver, and snap-froze tissues in liquid nitrogen and stored them at −80 °C prior to RNA or chromatin extraction. All procedures involving animals were conducted under an approved animal use protocol (PRO00006809) in accordance with the guidelines of the Institutional Animal Care and Use Committee at the University of Michigan.

Plasmids

The pSFV-*Dbp*-luc plasmid is a luciferase reporter vector that contains a 9.6-kb genomic fragment encompassing the entire mouse *Dbp* gene, plus 0.5 and 0.6 kb of 5′ and 3′ flanking region, respectively (Stratmann et al., 2012; provided by Dr. Ueli Schibler, University of Geneva). The pGL3–7.5 kb-*Klf9* luciferase reporter vector is described in Bagamasbad et al. (2015). The pShuttle-*Bmal1*, pShuttle-*Clock*, and pShuttle-*Per1* expression vectors were provided by Dr. Lei Yin (University of Michigan). Luciferase activity was normalized by cotransfection with the promoter-less pRL Renilla luciferase vector (Promega, Madison, WI). To construct the pCS2-*Klf9* expression vector, we used polymerase chain reaction (PCR) to amplify the full-length cDNA for rat *Klf9* using the pRSV-BTEB plasmid as a template (Kobayashi et al., 1995; gift of Dr. Yoshiaki Fujii-Kuriyama, Tokyo Medical and Dental University) and directionally subcloned the DNA fragment into pCS2. To construct the pcDNA4:TO-*Klf13* expression vector, we used pCMV-Entry-*Klf13* (MR224297; OriGene, Rockville, MD) as template to PCR amplify the *Klf13* open reading frame, then we directionally subcloned this DNA fragment into the pCDNA4:TO vector (Invitrogen, Carlsbad, CA; in the absence of the tet repressor, this is a constitutive expression vector). To construct pGL4.23-Dbp_{200}, we used PCR to generate a 200-bp DNA fragment located within the first intron of mouse *Dbp* using pSFV-*Dbp*-luc as a template and directionally subcloned it into the luciferase reporter plasmid pGL4.23 (Promega). We used this plasmid as a template to generate the pGL4.23-Dbp_{200} GC Box 1 mutant, pGL4.23-Dbp_{200} GC Box 2 mutant, and pGL4.23-Dbp_{200} double mutant vectors by site-directed mutagenesis using the Quick-Change kit (Agilent, Santa Clara, CA). All

oligonucleotide sequences used for PCR amplification and site-directed mutagenesis are given in Supplemental Table S1.

Cell Culture and transfection assays

We used HT22 cells, an adult mouse hippocampus-derived cell line immortalized with the SV40 T antigen that displays properties of differentiated neurons (Morimoto and Koshland, 1990b; Morimoto and Koshland, 1990a; Maher and Davis, 1996; Sagara et al., 1998). We also used HT22 cells that we previously (1) engineered to express a *Klf9* transgene under the control of the tetracycline repressor (i.e., *Klf9* mRNA is induced by treatment with doxycycline [Dox]; HT22[TR/TO-*Klf9*]), (2) engineered to co-express biotin ligase and a KLF9 fusion protein containing an N-terminal biotin ligase recognition peptide that becomes biotinylated in vivo (HT22[BirA/FLBIO-*Klf9*]), or (3) made deficient for *Klf9* using CRISPR/Cas9 genome editing (HT22[*Klf9* CRISPR]). We also used HEK293 cells for transfection assays. We cultured cells in high-glucose DMEM (Invitrogen) supplemented with 10% fetal bovine serum (FBS; Hyclone or Sigma, St. Louis, MO), penicillin G (100 U/mL), and streptomycin sulfate (100 μg/mL). We cultured cells under a humidified atmosphere of 5% CO_2 at 37 °C. We transfected cells using Fugene 6 (Promega) at a mass:volume ratio of 3:1 following the manufacturer's instructions.

To synchronize the cellular circadian clock of HT22 cells for analysis of gene expression and KLF9 recruitment to chromatin, we treated cells with the glucocorticoid corticosterone (CORT; Sigma) following the method of Balsalobre and colleagues (1998, 2000). For gene expression analysis, we plated 5×10^5 cells in 6-well plates in DMEM containing 1% FBS that was stripped of steroids using charcoal extraction as described (Yao et al., 2008). We synchronized cells by replacing the medium with serum-free DMEM containing 1 μM CORT and continued culturing for 1 h; controls received an equivalent volume of 100% ethanol (final concentration 0.05%). Cells were washed once with serum-free medium and then cultured in DMEM containing 10% steroid-stripped FBS. This procedure was begun 24 h after cell plating and repeated every 4 or 6 h on a new set of wells over a 42-, 48-, or 66-h period (n = 3–6/wells per treatment). At 42, 48, or 66 h, we harvested cells from all wells for RNA extraction and real-time quantitative PCR (RT-qPCR).

To analyze circadian variation in KLF9 association in chromatin in tissue culture cells, we plated 5×10^6 HT22 cells in 100-mm plates or 1×10^5 in 12-well plates in DMEM with 1% steroid-stripped FBS and then treated cells with CORT for 1-h intervals as described above, except that treatments were given every 4 h over the course of 24 h, starting 24 h after plating. Cells were harvested beginning at 18 h and continuing through 42 h after CORT treatment. At the end of the time course, we harvested cells for chromatin extraction (100-mm plates; n = 3 plates/time point) or RNA extraction (12-well plates; n = 4 wells/time point).

Rna extraction, Reverse transcription, and Rt-qPCR

We extracted total RNA from HT22 cells, mouse hippocampus, and liver using the TRIzol reagent (Invitrogen) according to the manufacturer's instructions. We treated the RNA with DNase 1 (20U; Roche, Basel, Switzerland) to remove genomic DNA, then

reverse transcribed 1 μg of RNA using the High Capacity Reverse Transcription kit with ribonuclease inhibitor from Applied Biosystems (Life Technologies Corp, Carlsbad, CA). For RT-qPCR, we used Taqman assays for *Gapdh* and *Klf9* (Bagamasbad et al., 2015) and SYBR green for all other assays. All oligonucleotide primer sequences are given in Supplemental Table S1. We conducted RT-qPCR using an ABI 7500 fast RT-PCR machine with Absolute qPCR low ROX mix or Absolute qPCR SYBR low ROX mix (ABgene, Portsmouth, NH). We designed SYBR assays using Integrated DNA Technology's RealTime qPCR Assay tool; all RT-qPCR assays were designed to span an exon-exon boundary. Standard curves were constructed by pooling cDNA from all samples and making serial 10-fold dilutions. The mRNA levels were normalized to the mRNAs of the reference genes *Gapdh* (HT22 and hippocampus) or *Ppia* (HT22 and liver).

Chromatin extraction and immunoprecipitation

We extracted chromatin from cells and mouse tissues and conducted a ChIP assay as described previously (Denver and Williamson, 2009; Bagamasbad et al., 2015; Knoedler et al., 2017), except that we sonicated DNA to 500- to 600-bp fragments using a Covaris S220 focused ultrasonicator (Covaris, Woburn, MA). For each ChIP reaction, we used 5 μg purified immunoglobulin G (IgG) from goat anti-mBTEB-C17 or normal goat IgG (both from Santa Cruz Biosciences, Santa Cruz, CA). We conducted relative quantification of the immunoprecipitated DNA using SYBR Green assays, with standard curves generated using a pool of input chromatin, and we normalized the KLF9 ChIP signal to the signal obtained with normal goat IgG.

Dual Luciferase assay

For transfection-reporter assays using HT22[TR/TO-*Klf9*], we plated cells in 24-well plates at a density of 5×10^4 cells/well. Twenty-four hours after plating, we transfected cells with 200 ng/well of one of the luciferase reporter vectors plus 10 ng of pRenilla plasmid (Invitrogen) to monitor transfection efficiency. Twenty-four hours after transfection, we treated cells with or without 1 μg/mL Dox for 12 h, after which time we harvested the cells for dual luciferase assay.

For dual luciferase assays using HEK293 cells, we cultured cells in 24-well plates at a density of 5×10^4 cells/well. Twenty four hours after plating, we transfected cells with 100 ng/well of luciferase reporter vectors containing mouse genomic regions with putative KLF9 binding sites (pGL3–7.5 kb-*Klf9*, pSFV-*Dbp*-Luc, pGL4.23-Dbp_{200}bp), 10 ng of pRenilla, and pCS2-*Klf9* (0.1, 1, or 10 ng per well), pShuttle-*Clock* and pShuttle-*Bmal1* (each plasmid at 0, 1, 3, 10, 30, or 100 ng/well for the dose-response experiment, 15 ng/ well for all other experiments), and pShuttle-*Per1* (0, 1, 3, 10, 30, or 60 ng/well for the dose-response experiment, 30 ng/well for all other experiments). The total plasmid DNA amount used per well was normalized using the pCS2-empty vector. We quantified luciferase activity using the Dual Luciferase Reporter Assay System (Promega) according to the manufacturer's instructions. We quantified firefly luciferase activity using a luminometer (Femtometer FB 12; Zylux Corp., Irvine, CA) and divided this by Renilla luciferase activity to give the relative luciferase activity (RLA). All transfection-reporter assays were repeated at least twice with 5 to 6 replicates/treatment.

Generation of ht22 Knockout Cell Lines Using CRisPR/Cas9 Genome editing

We used CRISPR/Cas9 genome editing to generate HT22 cells with inactivating mutations in *Klf13*, or *Klf9* and *Klf13*; *Klf9* single knockout HT22 cells were produced by us previously (Knoedler et al., 2017). To mutate the *Klf13* gene, we designed a guide RNA (gRNA) using 2 web tools: https://zlab.bio/guide-design-resoucers and https://chopchop.cbu.uib.no. We selected the sequence 5′ gcg cgg tcg tgc acg agc cg 3′, which was predicted by both algorithms and targets a sequence in the 5′ region of the *Klf13* gene. We purchased the custom pCas-*Klf-13*gRNA-EF1a-GFP plasmid from OriGene. We cultured the HT22 parent line in 10-cm tissue culture dishes and transfected cells with 5 μg of pCas-*Klf-13*gRNA-EF1a-GFP plasmid using Fugene 6. Twenty-four hours after transfection, we harvested cells and conducted fluorescence-assisted cell sorting (University of Michigan Flow Cytometry Core) to give 1 cell/well of a 96-well tissue culture plate. We expanded 8 individual clonal lines and screened for mutations at the region targeted by the *Klf13* gRNA. We cultured cells in 6-well plates, then harvested them and purified the genomic DNA using the DNeasy Blood & Tissue Kit (Qiagen, Hilden, Germany); this DNA was used as a template to amplify the region corresponding to that targeted by the *Klf13* gRNA. We subcloned the PCR products into the pGEMT-easy vector, then sequenced DNA isolated from at least 10 bacterial colonies per clonal HT22 cell line. For our experiments, we used a clonal line (designated HT22 Klf13-KO) that harbors mutations in 4 alleles (HT22 appears aneuploid; S. Raj, A. Subramani, and R. J. Denver, unpublished data) that generate several truncated forms of KLF13 containing the first 23 to 27 amino acids (Suppl. Fig. S1). To generate a double knockout Klf9 + Klf13 HT22 cell line, we transfected HT22 Klf13-KO cells with the plasmid pCas-Klf9gRNA-EF1a-GFP, which encodes the gRNA sequence 5′ ggg ggc gct ccg gaa gcc gac 3′ that targets the *Klf9* gene (Knoedler et al., 2017). Individual clones were selected, expanded, and characterized as described above. For our experiments, we used a clonal double knockout line (designated HT22 Klf9+Klf13 KO), in which a predicted truncated KLF9 protein containing the first 21 amino acids is generated for all alleles (Suppl. Fig. S1).

Identification of KLF13 Genomic targets Using Chromatin streptavidin Precipitation sequencing

We expressed a biotinylated form of KLF13 in the HT22-BirA cell line, then conducted ChSP-seq as described previously (Knoedler et al., 2017) with minor modifications. Here we used HT22 cells that we previously engineered to express the *Escherichia coli* biotin ligase BirA (HT22 [BirA]). We conducted transient transfections using Fugene 6 with pEF1α-FLBIO-Klf13, a plasmid that expresses KLF13 fused to a C-terminal FLAG tag and biotin ligase recognition peptide (Kim et al., 2009). As for KLF9 (Knoedler et al., 2017), this allowed for high-affinity purification of KLF13 by ChSP. Twenty-four hours after transfection, we isolated chromatin, cross-linked with formaldehyde, fragmented the genomic DNA by sonication, then precipitated the DNA-protein complexes using MyOne T1 streptavidin-conjugated Dynabeads (Invitrogen) as described previously (Knoedler et al., 2017). We used the purified DNA (at least 5 ng per sample) to prepare libraries from 4 streptavidin-precipitated samples and 4 inputs using the SMARTer ThruPLEX DNA-Seq Kit (Takara, Kyoto, Japan), and we sequenced all libraries (50-bp single end) in a single lane of an Illumina 4000 Hi-Seq machine at the University of Michigan DNA Sequencing

Core. We analyzed data quality using FastQC, then we mapped sequences to the reference mouse genome (mm10) using BWAmem. Additional quality controls for enrichment were conducted (deepTools, phantompeakqualtools, calculateNSCRSC.r, ngsplot) before calling peaks using PePr, and we then assigned genes to enriched peaks using ChIPseeker. The regions of the circadian clock genes where KLF13 associates were visualized using the Integrative Genome Viewer (Broad Institute). Full details of the experimental procedures and the complete data sets generated by KLF13 ChSP-seq will be published in a separate article.

Data analysis and statistics

We analyzed data by Student's unpaired *t* test or one-way analysis of variance (ANOVA) with Holm-Sidak or Fisher's least significant difference post hoc tests using Sigmaplot 13.0 or Systat 13 (Systat Software, San Jose, CA). Derived values were $\log_{10}$-transformed prior to statistical analysis if the variance was found to be heterogeneous. We analyzed circadian oscillations in gene expression by first linearly detrending the data using the least-squares method before conducting cosine fitting using CircWave software (https://www.euclock.org/results/item/circ-wave.html).

RESULTS

KLF9 associates in Chromatin at Circadian Clock Genes in ht22 Cells and in adult Mouse hippocampus

We recently published a genome-wide analysis of KLF9 association in chromatin in HT22 cells expressing a biotinylated KLF9 fusion protein using ChSP-seq (Kim et al., 2009; Knoedler et al., 2017). We found that KLF9 associated in chromatin within 10 kb upstream of TSSs and/or within introns of 10 genes that function in the cellular circadian oscillator. These included the core loop genes *Per1* and *Per3*, the accessory loop genes *Nr1d1* and *Nr1d2*, the autofeedback loop genes *Bhelhe40* and *Bhlhe41*, the loop-modulating kinase *Csnk1d*, and the clock-output genes *Dbp*, *Tef*, and *Wee1* (Fig. 1A, B). Among these 10 circadian clock genes, we found 13 distinct KLF9 ChSP-seq peaks. The DNA sequence underlying each peak contained at least one consensus KLF9 binding site (Knoedler et al., 2017), and 12 of these regions also had E-box-like motifs predicted by HOMER, which are consensus CLOCK+BMAL1 binding sites (Gekakis et al., 1998). Nine of the 13 KLF9 peaks near circadian clock genes overlapped with CLOCK ChIP-seq peaks that were previously identified in mouse liver (Yoshitane et al., 2014). Of the 3514 KLF9 ChSP-seq peaks that we found in HT22 cells, 1028 (29%) contain E-boxes. De novo motif discovery using HOMER found that E-box motifs were more common within KLF9 peaks than would be expected by chance ($p < 1 \times 10^{-28}$). Targeted ChIP assays at regions of KLF9 peaks identified in HT22 cells by ChSP-seq at 3 clock-output genes confirmed that KLF9 associates in chromatin from mouse hippocampus at *Dbp*, *Tef*, and *Wee1* (Fig. 1C).

Klf9 mRna Level in Mouse Hippocampus and Liver Varies over a 20-h Period, and *Klf9* transcription is Regulated by CLOCK+BMaL1

The *Klf9* mRNA level displayed circadian oscillation in human keratinocytes and in mouse liver (Sporl et al., 2012; Yoshitane et al., 2014). We measured *Klf9* mRNA in male C57BL/6

mice killed every 4 h over a 20-h period (ZT2-ZT22). *Klf9* mRNA showed statistically significant variation over the course of the day in hippocampus (Fig. 2A; hippocampus: $F_{5,15} = 4.279$, $p = 0.013$); we also saw variation in *Klf9* mRNA in liver (Suppl. Fig. S2). In human keratinocytes and in mouse liver, CLOCK associates in chromatin near E-boxes in the 5′ upstream *Klf9* flanking region (Sporl et al., 2012; Yoshitane et al., 2014). This region, located −5.33 to −5.15 kb from the mouse TSS, contains an ultraconserved super enhancer that binds nuclear receptors, among other transcription factors, and mediates hormone action on *Klf9* transcription (the *Klf9* synergy module [KSM]; Bagamasbad et al., 2015). The mouse liver CLOCK ChIP peak, within which is a consensus E-box, is found immediately upstream of the mouse KSM at −5.36 kb (Yoshitane et al., 2014). We looked at whether the mouse *Klf9* upstream flanking region can support transcriptional activation by CLOCK+BMAL1 by co-transfecting HT22 and HEK293 cells with the luciferase reporter vector pGL3–7.5kb-*Klf9*, which contains a DNA fragment corresponding to 7.5 kb upstream of the mouse *Klf9* TSS, plus the expression vectors pShuttle-*Clock* and pShuttle-*Bmal1.* Pilot experiments showed that although the cell lines behaved similarly, HEK293 cells showed greater CLOCK+BMAL1-dependent promoter activation, so we used this line for subsequent experiments. Forced expression of *Clock* plus *Bmal1* increased RLA driven by the *Klf9* upstream flanking region, which was abrogated by co-transfection with pShuttle-*Per1* (Fig. 2B).

KLF9 association in Chromatin exhibits Circadian Oscillation in ht22 Cells, and KLF9 Represses Clock-output Gene transcription

To investigate whether KLF9 plays a role in modulating the cellular circadian clock, we first synchronized circadian clock gene transcription in HT22 cells by treating with 1 μM CORT for 1 h (Balsalobre et al., 1998, 2000); control cells received EtOH vehicle. We then used RT-qPCR to analyze mRNA levels for *Klf9*, the core circadian clock gene *Per2*, and the clock-output gene *Dbp* at 6-h intervals for 48 h. The *Klf9* mRNA (Fig. 2C) and the *Dbp* and *Per2* mRNAs (Suppl. Fig. S3) exhibited circadian oscillation in the CORT but not in vehicle-treated cells.

To determine if KLF9 association in chromatin undergoes circadian changes, we synchronized HT22 cells as above, harvested chromatin at 4-h intervals for 20 h, then conducted ChIP assays for KLF9, targeting the first *Dbp* intron where KLF9 associates (the first peak, left to right, shown in Fig. 1B). At the same time, we harvested RNA from identically treated cells to investigate changes in *Dbp* mRNA. We saw the peak KLF9 association in chromatin at the *Dbp* locus at 34 h after CORT, which coincided with the minimum *Dbp* mRNA level (Fig. 2D). Peak *Dbp* mRNA level was seen at 28 h after CORT, which coincided with the nadir of KLF9 association in chromatin (Fig. 2D).

Our findings in HT22 cells, in which KLF9 association in chromatin underwent circadian oscillation in antiphase to the *Dbp* mRNA level, prompted us to hypothesize that KLF9 functions as a repressor of *Dbp* transcription. Our previous work showed that KLF9 functions predominantly as a transcriptional repressor in neurons (Knoedler et al., 2017). To test this, we used the tetracycline-inducible cell line HT22[TR/ TO-*Klf9*] (Knoedler et al., 2017) to determine if forced expression of *Klf9* can modulate the *Dbp* mRNA level.

Six hours of Dox treatment, which causes a 6-fold increase in *Klf9* mRNA (Knoedler et al., 2017), reduced the *Dbp* mRNA level by ~50% compared with vehicle-treated HT22[TR/TO-*Klf9*] cells (Fig. 2E). Also, two clonal HT22 cell lines in which we deleted *Klf9* using CRISPR/Cas9 genome editing (Knoedler et al., 2017) showed a 2.3-fold increase in the *Dbp* mRNA level (Fig. 2F).

Forced expression of KLF9 antagonizes CLOCK+BMaL1 activation of *Dbp* transcription

Dbp is a clock-output gene that shows >160-fold oscillation in protein level over the course of the day in mouse liver (Ripperger and Schibler, 2006). The circadian core loop transcription factors CLOCK and BMAL1 undergo rhythmic association in chromatin by binding to E-boxes at multiple regions of the *Dbp* locus, which is hypothesized to lead to circadian changes in *Dbp* transcription (Ripperger et al., 2000; Ripperger and Schibler, 2006). A region within the first intron of *Dbp* contains an E-box that overlaps with a KLF9 peak that we identified previously by ChSP-seq (Knoedler et al., 2017; Fig. 3A). We therefore investigated whether KLF9 can modulate CLOCK+BMAL1-dependent *Dbp* transcription by transient transfection assay using pSFV-*Dbp*-luc. This reporter vector, which contains the entire mouse *Dbp* gene, supports circadian oscillation in luciferase activity when transfected into synchronized NIH 3T3 cells (Stratmann et al., 2012). We found that co-transfection of HEK293 cells with different amounts of the expression vectors for *Clock* and *Bmal1* increased the RLA supported by the pSFV-*Dbp*-luc vector (Suppl. Fig. S4A). Conversely, co-transfection with pShuttle-*Per1* caused a dose-dependent inhibition of CLOCK+BMAL1 activation of pSFV-*Dbp*-luc (15 ng plasmid each of pShuttle-*Bmal1* plus pShuttle-*Clock*; Suppl. Fig. S4B). The HEK293 cells showed stronger responses to CLOCK+BMAL1 than HT22 (7-fold vs. 1.6-fold activation of pSFV-*Dbp*-luc in HEK293 vs. HT22, respectively), so for all subsequent experiments, we used HEK293 cells.

To determine if KLF9 can influence CLOCK+BMAL1 transcriptional activity, we co-transfected HEK293 cells with pSFV-*Dbp*-luc, pShuttle-*Clock* plus pShuttle-*Bmal1* (15 ng each), and varying amounts of pCS2-*Klf9*. Forced expression of *Klf9* alone (i.e., without pShuttle-*Bmal1* plus pShuttle-*Clock*) caused a dose-dependent decrease in the RLA, with the maximum dose (10 ng) reducing RLA by 65% (Fig. 3B). Co-transfection of pShuttle-*Bmal1* plus pShuttle-*Clock* without pCS2-*Klf9* caused a 3.1-fold increase in RLA, whereas co-transfection with pCS2-*Klf9* (at the 1- and 10-ng plasmid doses) abolished the CLOCK+BMAL1-dependent activation of the *Dbp* reporter (Fig. 3B).

We also tested whether KLF9 can act synergistically with PER1 to inhibit CLOCK+BMAL1 transactivation. Co-transfection of pShuttle-*Bmal1* plus pShuttle-*Clock* caused a 6.75-fold increase in RLA from pSFV-*Dbp*-luc, which was reduced by 26% by co-transfection with pShuttle-*Per1* (Fig. 3C). Transfection with pCS2-*Klf9* caused a dose-dependent decrease in CLOCK+BMAL1-induced RLA, but this action was not affected by co-transfection with pShuttle-*Per1* (Fig. 3C).

Interference of CLOCK+BMaL1 transcriptional activity by KLF9 Requires intact GC Boxes within the *Dbp* intron

Our previous ChSP-seq experiment identified a set of partially redundant, GC-rich motifs (GC-boxes) present in 98% of all KLF9 peaks (Knoedler et al., 2017). We found 2 such motifs located in close proximity to the E-box within the first *Dbp* intron, and like the E-box, both putative KLF9 binding sites are conserved among eutherian mammals (Fig. 4A; Ripperger and Schibler, 2006). To investigate if one or both GC boxes play a role in *Dbp* transcriptional repression by KLF9, we isolated a 200-bp region corresponding to the KLF9 peak within the first *Dbp* intron (see Fig. 1B) and then subcloned it to generate the luciferase reporter vector pGL4.23-Dbp_{200} for analysis in the transient transfection assay. We also used site-directed mutagenesis to change the 7 nucleotides that comprise each GC box to thymidine, making either single or double GC box mutants. Expression of CLOCK+BMAL1 increased the RLA supported by wild-type pGL4.23-Dbp_{200} by 5-fold (Fig. 4B), which was similar to the full-length *Dbp* reporter construct pSFV-*Dbp*-luc (see Fig. 3B, C). Co-transfection with pCS2-*Klf9* reduced the baseline RLA by 50% and the CLOCK+BMAL1-dependent increase by 70%. Mutation of either GC box alone eliminated KLF9 repression of baseline reporter activity and reduced, but did not eliminate, KLF9 repression of CLOCK+BMAL1 activity (KLF9 caused a 21% reduction in the GC box 1 mutant, and 36% in the GC box 2 mutant; Fig. 4B). The KLF9 repression of both baseline and CLOCK+BMAL1-dependent reporter activity was eliminated in the double GC box mutant (Fig. 4B).

KLF9 association in Chromatin in the hippocampus at the *Dbp* Locus Varies over a 20-h Period

Using targeted ChIP assays, we found a statistically significant variation in KLF9 association within the first intron of *Dbp* in chromatin isolated from mouse hippocampus over a 20-h period (Suppl. Fig. S5). The mean KLF9 ChIP signal reached a maximum at ZT6 and a trough at ZT18, which was paralleled by changes in *Dbp* mRNA and heteronuclear RNA (hnRNA is a measure of active gene transcription; Suppl. Fig. S5).

Loss of KLF9 and KLF13 in ht22 Cells Disrupts *Dbp* Oscillation

We next tested whether loss of KLF9 alters the circadian rhythm in *Dbp* mRNA in HT22 cells. We used *Klf9* KO HT22 cells (Knoedler et al., 2017) and followed the cell synchronization protocol described above. As before, the HT22 parent cell line showed a statistically significant circadian oscillation in *Dbp* mRNA, but the mutation of *Klf9* had no effect on this rhythmicity (Fig. 5). Vertebrate *Klf9* and *Klf13* genes are paralogous (Kaczynski et al., 2003); they share 63% sequence similarity. Based on their relatedness, and that previous work from the Simmen Laboratory showed that these 2 KLFs have some overlapping functions in the mouse uterus (Heard et al., 2012; Heard et al., 2015), we hypothesized that KLF13 can compensate for the loss of KLF9. As for *Klf9*, mutation of *Klf13* alone did not affect the *Dbp* mRNA rhythm. By contrast, regular oscillations in *Dbp* mRNA were abolished in the double knockout cells (Fig. 5). We also analyzed 3 core clock genes (*PerIII*, a target of KLF9 and KLF13 based on our ChSP-seq analyses; *Cry1*, a target of KLF13; and *PerII*, not a target of either KLF). There was no statistically significant

oscillation in *PerIII* or *Cry1* mRNAs in the wild-type cells; however, like *Dbp*, double *Klf* gene knockout markedly reduced the overall mRNA level for both genes (Suppl. Figs. S6 and S7). For *PerII*, which is not a direct target of KLF9 or KLF13, the overall mRNA level was largely unaffected by KLF gene knockout (Suppl. Fig. S8; however, double *Klf* gene knockout disrupted the circadian oscillation of *PerII* mRNA, perhaps because of the loss of indirect actions of the two KLFs on this gene). The mRNA level of the reference gene *Ppia* was similar among the 4 genotypes and showed no statistically significant variation over the course of the experiment (Suppl. Fig. S9), supporting that there was no general suppression of gene expression in the double knockout cells to explain the overall reduction in *Dbp, Cry1*, and *PerIII* mRNA levels.

We also tested whether an impaired response to CORT (that we used to synchronize the cells) in the *Klf* gene knockout cells was responsible for the disruption of the circadian oscillation in gene expression. Treatment with CORT for 1 or 4 h caused a similar induction of *PerI* mRNA (*Per1* is a direct GR target gene that is rapidly and strongly induced by CORT; Yamamoto et al., 2005; Reddy et al., 2012) in all 4 genotypes (Suppl. Fig. S10), supporting that the disrupted gene expression was not due to an impaired response to CORT.

KLF13 Regulates Components of the Cellular Circadian Clock, some Overlapping with KLF9 targets

The loss of *Dbp* circadian rhythmicity in double mutant *Klf9+Klf13* cells prompted us to investigate whether KLF13 might regulate cellular circadian clock genes. The DNA binding domains of KLF9 and KLF13 are highly similar, and they share N-terminal functional domains. We looked at KLF13 ChSP-sequencing data from HT22 cells (J. Ávila-Mendoza and R. J. Denver, unpublished data) and found KLF13 associated in chromatin at 11 cellular clock genes (Fig. 6A); there were peaks for both KLF9 and KLF13 at 8 of these 11 genes (Figs. 1A and 6A). Target genes that differed between the 2 transcription factors were *Per1* and *Nr1d1* (KLF9 only) and *Csnk1e*, *Cry1*, and *Cry2* (KLF13 only). The KLF9 and KLF13 ChSP-seq peaks overlapped at *Per3*, *Nr1d2*, *Bhlhe40*, *Tef*, and *Wee1*; at *Dbp*, the KLF13 peak overlapped with one of the KLF9 peaks found at the second exon/intron boundary but not the KLF9 peak at the first intron, which contains a canonical CLOCK/BMAL1 binding site. At the *Bhlhe41* locus, while a single KLF9 peak was found in the 5′ flanking region overlapping with a CLOCK/BMAL1 binding site, 2 KLF13 peaks were found overlapping with the first and fourth exons at the 5′ end of the gene. A targeted ChIP assay using a custom polyclonal anti-KLF13 serum showed that KLF13 associated in chromatin from the mouse hippocampus at the *Dbp*, *Tef*, and *Wee1* loci, similar to KLF9 (Fig. 6B). Lastly, in transient transfection assays in HEK293 cells, forced expression of *Klf13* caused a dose-dependent repression of baseline transcription from the pSFV-Dbp-luc reporter vector and also blocked activation of this reporter by co-expression of CLOCK/BMAL1 (Fig. 6C). Unlike *Klf9*, the *Klf13* mRNA did not exhibit circadian oscillation in HT22 cells or mouse hippocampus (Suppl. Fig. S11).

DISCUSSION

Here we show that *Klf9* is a clock-output gene, and KLF9 genomic targets include key clock and clock-output genes. We found that KLF9 associates in chromatin at 10 genes that form the core circadian TTFL, and its association at the clock-output gene *Dbp* showed circadian variation in HT22 cells and mouse hippocampus. Forced expression of KLF9 reduced) whereas loss of KLF9 increased the *Dbp* mRNA level in HT22 cells. In addition, KLF9 strongly inhibited CLOCK+BMAL1-dependent *Dbp* transactivation, while mutation of two GC boxes within the first *Dbp* intron eliminated KLF9-dependent repression, supporting that this action requires direct DNA binding by KLF9. Our findings support that KLF9 functions within multiple arms of the cellular circadian clock and therefore may play a central role in modulating circadian clock output. We also provide evidence that the paralogous transcription factor KLF13 may compensate for the loss of KLF9 in regulating circadian gene expression and vice versa. KLF13 associated in chromatin at several core clock and clock output genes, 8 that overlapped with KLF9. Furthermore, KLF13, like KLF9, strongly inhibited CLOCK+BMAL1-dependent *Dbp* transactivation.

Our finding that *Klf9* mRNA undergoes circadian oscillation in CORT-synchronized HT22 cells, and varies over a 20-h period in hippocampus and liver, agree with data of Yoshitane and colleagues (2014) as well as Spörl and colleagues (2012), who found circadian changes in *Klf9* mRNA in mouse liver and in human keratinocytes, respectively. This regulatory pattern may be explained by CLOCK+BMAL1 binding to a canonical E-box at 5.26 kb upstream of the *Klf9* TSS, which is immediately upstream of the KSM (Sporl et al., 2012; Yoshitane et al., 2014; Bagamasbad et al., 2015). Using transfection/reporter assays, we show that CLOCK+BMAL1 can activate transcription from the *Klf9* 5′ flanking region, which was blocked by co-expression of PER1. Taken together, the data support that *Klf9* is a clock-output gene. A previous genome-wide study conducted on mouse liver chromatin showed that 6 of 17 members of the *Klf* gene family (9, 10, 11, 13, 15, and 16) are genomic targets of CLOCK+BMAL1, and each of the mRNAs for these genes showed circadian oscillation (Yoshitane et al., 2014). Other studies have shown that KLFs mediate circadian variation in gene expression and physiological outputs (Guillaumond et al., 2010; Jeyaraj et al., 2012a; Jeyaraj et al., 2012b; Han et al., 2015). However, to our knowledge, no studies have shown that members of the KLF family directly affect the function or output of the core cellular circadian oscillator.

Our previous ChSP-seq study found that KLF9's genomic targets include multiple clock- and clock-output genes, suggesting that KLF9 may play a role in circadian gene regulation. Here we focused our investigations on the clock-output gene *Dbp*. In HT22 cells, changes in KLF9 recruitment to chromatin at the *Dbp* locus and *Dbp* mRNA were in antiphase, which may reflect a negative regulatory relationship. In support of a repressive action of KLF9 on *Dbp*, we found that forced *Klf9* expression in HT22 cells reduced, whereas loss of KLF9 increased *Dbp* mRNA level. Our promoter-reporter assays showed that KLF9 strongly inhibited CLOCK+BMAL1 activation of *Dbp* transcription. Furthermore, the full repressor activity of KLF9 on a 200-bp region corresponding to the *Dbp* first intron, where we previously showed that KLF9 associates in chromatin, required the presence of 2 intact consensus KLF9 binding sites. To our knowledge, this is the first demonstration of the

inhibition of the transcriptional activity of CLOCK+BMAL1 by a GC box binding factor. The CLOCK+BMAL1 complex is known to exhibit rhythmic association with multiple E-box elements located within the *Dbp* gene and activates transcription at this locus (Stratmann et al., 2012). Furthermore, association of CLOCK+BMAL1 at *Dbp* correlates with rhythmic changes in chromatin modifications, with histone marks indicative of active genes accumulating during the active phase of transcription, and negative histone marks accumulating when the gene is repressed (Ripperger and Schibler, 2006). KLF9 may play a key role in modulating CLOCK/BMAL1 action and generating a repressive chromatin state at *Dbp* and perhaps at other clock and clock-output genes. Notably, we found that approximately onethird of KLF9 ChSP-seq peaks in HT22 cells also contain E-boxes. Transcriptional antagonism by GC box binding factors may be a general mechanism for fine-tuning or providing tissue- or cell-type specificity to circadian gene regulation.

Our targeted ChIP assays showed variation in KLF9 association in chromatin at the *Dbp* locus in mouse hippocampus over a 20-h period. However, in contrast to HT22 cells, these changes largely paralleled changes in *Dbp* mRNA and heteronuclear RNA (Suppl. Fig. S5). These findings support that KLF9 undergoes rhythmic association with *Dbp* in mouse brain in vivo, but they do not provide support for KLF9 acting as a repressor of *Dbp*. It is possible that peak KLF9 association in chromatin at *Dbp*, corresponding to the peak in *Dbp* mRNA, leads to the initiation and/or support of the subsequent decline in transcription through recruitment of chromatin modifiers to generate a repressive chromatin state (e.g., the repressor protein SIN3A; Zhang et al., 2001) or the inhibition of CLOCK+BMAL1 activity, as we found in HT22 cells.

When we knocked out *Klf9* alone in HT22 cells, we saw no effect on *Dbp* rhythmicity. We hypothesized that the closely related KLF13 might compensate for loss of KLF9; in mouse uterus, KLF9 and KLF13 have partially overlapping functions in mediating the decidualization of endometrial stromal cells in response to progesterone (Heard et al., 2012; Heard et al., 2015). We therefore knocked out *Klf13* alone, or *Klf9*+*Klf13*, but only the double gene knockout caused a phenotype, which was the complete loss of *Dbp* mRNA rhythmicity. We also found that KLF13 associates in chromatin at clock and clock-output genes, 8 of which are shared with KLF9, and like KLF9, KLF13 can strongly repress CLOCK-BMAL1-dependent transactivation of *Dbp*. Our findings support that, together, these 2 KLFs play an essential, cooperative role in regulating *Dbp* transcription. However, this function cannot be explained by simple gene repression, but may involve a more complex role for these transcription factors in modulating chromatin state at this locus, thereby allowing the gene to be expressed in a circadian manner. The mechanism for this cooperation requires further investigation. It is noteworthy that both KLF9 and KLF13 can activate and repress gene transcription, but why some genes are activated while others are repressed is poorly understood (Philipsen and Suske, 1999; Pearson et al., 2008; Knoedler et al., 2017). We have seen similar cooperation among these two closely related transcription factors in other pathways that they co-regulate such as neuronal morphology (i.e., neurite outgrowth) and response to neuronal damage (i.e., regeneration; J. Ávila-Mendoza and R. J. Denver, unpublished data).

Lastly, both *Klf9* and *Klf13* are regulated by diverse extracellular signals, including oxidative and xenobiotic stress, and hormones such as glucocorticoids and thyroid hormone (Mannava et al., 2012; Zucker et al., 2014; Bagamasbad et al., 2015). Each of these factors is known to, or has the potential to modulate peripheral circadian clocks. There is mounting evidence that the SCN communicates with peripheral circadian clocks via modulation of the hypothalamo-pituitary-adrenal axis, which produces glucocorticoids that directly regulate the transcription of core clock genes (Dickmeis et al., 2013; Schibler et al., 2015). We previously showed that *Klf9* is strongly regulated by glucocorticoids in mouse hippocampus via 2 evolutionarily conserved GREs (Bagamasbad et al., 2012; Bagamasbad et al., 2015). Glucocorticoid regulation of *Klf13* via a GRE located in the first intron may play a critical role in the survival of cardiomyocytes (Cruz-Topete et al., 2016). These findings raise the interesting possibility that KLF9 and KLF13, perhaps in concert with PER1 and PER2, which are also strongly regulated by glucocorticoids (Yamamoto et al., 2005; Cheon et al., 2013), may modulate glucocorticoid action on the cellular circadian clock, and therefore play a role in synchronizing central and peripheral clocks.

In summary, our findings show that the paralogous transcription factors KLF9 and KLF13 can directly regulate the cellular circadian clock output gene *Dbp*. Both KLFs have the potential to regulate other clock output genes and also core clock genes. Importantly, they can strongly antagonize CLOCK+BMAL1 activity, which could influence many E-box containing genes, thereby altering the timing and amplitude of circadian oscillation of gene transcription and therefore cell physiology.

Supplementary Material

Refer to Web version on PubMed Central for supplementary material.

ACKNOWLEDGMENTS

The work presented in this article was supported by grant NINDS 1 R01 NS046690 to R.J.D. and NIH 1T32HD079342-01 and a MCubed grant to J.R.K. and R.J.D. The pSFV-Dbp-luc plasmid was a generous gift of Dr. Ueli Schibler (University of Geneva). The pShuttle-*Bmal1*, pShuttle-*Clock*, and pShuttle-*Per1* expression vectors were provided by Dr. Lei Yin (University of Michigan). Dr. David Schubert (Salk Institute, La Jolla, CA) provided the HT22 cells. Dr. Christopher Sifuentes (University of Michigan Bioinformatics Core) conducted the bioinformatics analysis for the KLF13 ChSP-seq experiment. Dr. Cristina Saenz de Miera Patin provided comments on the article.

REFERENCES

Abramowitz J, Yildirim E, and Birnbaumer L (2007) The TRPC family of ion channels: relation to the TRP superfamily and role in receptor- and store-operated calcium entry. In: Liedtke HS, editor, TRP Ion Channel Function in Sensory Transduction and Cellular Signaling Cascades. Boca Raton (FL): CRC Press. p. 1–30.

Avci HX, Lebrun C, Wehrle R, Doulazmi M, Chatonnet F, Morel M-P, Ema M, Vodjdani G, Sotelo C, Flamant F, et al. (2012) Thyroid hormone triggers the developmental loss of axonal regenerative capacity via thyroid hormone receptor alpha1 and kruppel-like factor 9 in Purkinje cells. Proc Natl Acad Sci U S A 109: 14206–14211.

Bagamasbad P, Bonett R, Sachs L, Buisine N, Raj S, Knoedler J, Kyono Y, Ruan Y, Ruan X, and Denver R (2015) Deciphering the regulatory logic of an ancient, ultraconserved nuclear receptor enhancer module. Mol Endocrinol 29:856–872. [PubMed: 25866873]

Bagamasbad P, Howdeshell KL, Sachs LM, Demeneix BA, and Denver RJ (2008) A role for basic transcription element-binding protein 1 (BTEB1) in the autoinduction of thyroid hormone receptor beta. J Biol Chem 283: 2275–2285. [PubMed: 18045867]

Bagamasbad P, Ziera T, Borden SA, Bonett RM, Rozeboom AM, Seasholtz A, and Denver RJ (2012) Molecular basis for glucocorticoid induction of the Kruppel-like factor 9 gene in hippocampal neurons. Endocrinology 153:5334–5345. [PubMed: 22962255]

Bagamasbad PD, Espina JEC, Knoedler JR, Subramani A, Harden AJ, and Denver RJ (2019) Coordinated transcriptional regulation by thyroid hormone and glucocorticoid interaction in adult mouse hippocampus-derived neuronal cells. PloS One 14:e0220378.

Balsalobre A, Brown SA, Marcacci L, Tronche F, Kellendonk C, Reichardt HM, Schütz G, and Schibler U (2000) Resetting of circadian time in peripheral tissues by glucocorticoid signaling. Science 289:2344–2347. [PubMed: 11009419]

Balsalobre A, Damiola F, and Schibler U (1998) A serum shock induces circadian gene expression in mammalian tissue culture cells. Cell 93:929–937. [PubMed: 9635423]

Carmona-Saez P, Chagoyen M, Tirado F, Carazo JM, and Pascual-Montano A (2007) GENECODIS: a web-based tool for finding significant concurrent annotations in gene lists. Genome Biol 8:R3. [PubMed: 17204154]

Cayrou C, Denver RJ, and Puymirat J (2002) Suppression of the basic transcription element-binding protein in brain neuronal cultures inhibits thyroid hormone-induced neurite branching. Endocrinology 143:2242–2249. [PubMed: 12021188]

Cheon S, Park N, Cho S, and Kim K (2013) Glucocorticoid-mediated Period2 induction delays the phase of circadian rhythm. Nucleic Acids Res 41:6161–6174. [PubMed: 23620290]

Cruz-Topete D, He B, Xu XJ, and Cidlowski JA (2016) Kruppel-like factor 13 is a major mediator of glucocorticoid receptor signaling in cardiomyocytes and protects these cells from DNA damage and death. J Biol Chem 291:19374–19386.

Dardente H and Cermakian N (2007) Molecular circadian rhythms in central and peripheral clocks in mammals. Chronobiol Int 24:195–213. [PubMed: 17453843]

Denver RJ, Ouellet L, Furling D, Kobayashi A, FujiiKuriyama Y, and Puymirat J (1999) Basic transcription element binding protein (BTEB) is a thyroid hormone-regulated gene in the developing central nervous system: evidence for a role in neurite outgrowth. J Biol Chem 274:23128–23134.

Denver RJ and Williamson KE (2009) Identification of a thyroid hormone response element in the mouse Kruppel-like factor 9 gene to explain its postnatal expression in the brain. Endocrinology 150:3935–3943. [PubMed: 19359381]

Dickmeis T, Weger BD, and Weger M (2013) The circadian clock and glucocorticoids—interactions across many time scales. Mol Cell Endocrinol 380:2–15. [PubMed: 23707790]

Etchegaray JP, Machida KK, Noton E, Constance CM, Dallmann R, Di Napoli MN, DeBruyne JP, Lambert CM, Yu EA, Reppert SM, et al. (2009) Casein kinase 1 delta regulates the pace of the mammalian circadian clock. Mol Cell Biol 29:3853–3866. [PubMed: 19414593]

Gachon F, Olela FF, Schaad O, Descombes P, and Schibler U (2006) The circadian PAR-domain basic leucine zipper transcription factors DBP, TEF, and HLF modulate basal and inducible xenobiotic detoxification. Cell Metab 4:25–36. [PubMed: 16814730]

Gekakis N, Staknis D, Nguyen HB, Davis FC, Wilsbacher LD, King DP, Takahashi JS, and Weitz CJ (1998) Role of the CLOCK protein in the mammalian circadian mechanism. Science 280:1564–1569. [PubMed: 9616112]

Griffin EA Jr., Staknis D, and Weitz CJ (1999) Lightindependent role of CRY1 and CRY2 in the mammalian circadian clock. Science 286:768–771. [PubMed: 10531061]

Guillaumond F, Grechez-Cassiau A, Subramaniam M, Brangolo S, Peteri-Brunback B, Staels B, Fievet C, Spelsberg TC, Delaunay F, and Teboul M (2010) Kruppel-like factor KLF10 is a link between the circadian clock and metabolism in liver. Mol Cell Biol 30:3059–3070. [PubMed: 20385766]

Han S, Zhang R, Jain R, Shi H, Zhang L, Zhou G, Sangwung P, Tugal D, Atkins GB, Prosdocimo DA, et al. (2015) Circadian control of bile acid synthesis by a KLF15Fgf15 axis. Nat Commun 6:7231. [PubMed: 26040986]

Heard ME, Pabona JMP, Clayberger C, Krensky AM, Simmen FA, and Simmen RCM (2012) The reproductive phenotype of mice null for transcription factor Kruppel-like factor 13 suggests compensatory function of family member Kruppel-like factor 9 in the peri-implantation uterus. Biol Reprod 87:115. [PubMed: 22993382]

Heard ME, Velarde MC, Giudice LC, Simmen FA, and Simmen RCM (2015) Kruppel-like factor 13 deficiency in uterine endometrial cells contributes to defective steroid hormone receptor signaling but not lesion establishment in a mouse model of endometriosis. Biol Reprod 92:140. [PubMed: 25904015]

Heinz S, Benner C, Spann N, Bertolino E, Lin YC, Laslo P, Cheng JX, Murre C, Singh H, and Glass CK (2010) Simple combinations of lineage-determining transcription factors prime cis-regulatory elements required for macrophage and B cell identities. Mol Cell 38:576–589. [PubMed: 20513432]

Honma S, Ikeda M, Abe H, Tanahashi Y, Namihira M, Honma K, and Nomura M (1998) Circadian oscillation of BMAL1, a partner of a mammalian clock gene Clock, in rat suprachiasmatic nucleus. Biochem Biophys Res Commun 250:83–87. [PubMed: 9735336]

Jeyaraj D, Haldar SM, Wan X, McCauley MD, Ripperger JA, Hu K, Lu Y, Eapen BL, Sharma N, Ficker E, et al. (2012a) Circadian rhythms govern cardiac repolarization and arrhythmogenesis. Nature 483:96–99. [PubMed: 22367544]

Jeyaraj D, Scheer FA, Ripperger JA, Haldar SM, Lu Y, Prosdocimo DA, Eapen SJ, Eapen BL, Cui Y, Mahabeleshwar GH, et al. (2012b) Klf15 orchestrates circadian nitrogen homeostasis. Cell Metab 15:311–323. [PubMed: 22405069]

Kaczynski J, Cook T, and Urrutia R (2003) Sp1-and Kruppel-like transcription factors. Genome Biol 4:209. [PubMed: 12620099]

Kawamoto T, Noshiro M, Sato F, Maemura K, Takeda N, Nagai R, Iwata T, Fujimoto K, Furukawa M, Miyazaki K, et al. (2004) A novel autofeedback loop of Dec1 transcription involved in circadian rhythm regulation. Biochem Biophys Res Commun 313:117–124. [PubMed: 14672706]

Kent WJ, Sugnet CW, Furey TS, Roskin KM, Pringle TH, Zahler AM, and Haussler D (2002) The human genome browser at UCSC. Genome Res 12:996–1006. [PubMed: 12045153]

Kim J, Cantor AB, Orkin SH, and Wang JL (2009) Use of in vivo biotinylation to study protein-protein and protein-DNA interactions in mouse embryonic stem cells. Nat Protoc 4:506–517. [PubMed: 19325547]

Knoedler JR, Subramani A, and Denver RJ (2017) The Kruppel-like factor 9 cistrome in mouse hippocampal neurons reveals predominant transcriptional repression via proximal promoter binding. BMC Genomics 18:299. [PubMed: 28407733]

Kobayashi A, Sogawa K, Imataka H, and Fujiikuriyama Y (1995) Analysis of functional domains of a GC box binding protein, BTEB. J Biochem 117:91–95. [PubMed: 7775404]

Leliavski A, Dumbell R, Ott V, and Oster H (2015) Adrenal clocks and the role of adrenal hormones in the regulation of circadian physiology. J Biol Rhythms 30:20–34. [PubMed: 25367898]

Maher P and Davis JB (1996) The role of monoamine metabolism in oxidative glutamate toxicity. J Neurosci 16:6394–6401. [PubMed: 8815918]

Mannava S, Zhuang D, Nair JR, Bansal R, Wawrzyniak JA, Zucker SN, Fink EE, Moparthy KC, Hu Q, and Liu S (2012) KLF9 is a novel transcriptional regulator of bortezomib- and LBH589-induced apoptosis in multiple myeloma cells. Blood 119:1450–1458. [PubMed: 22144178]

Morimoto BH and Koshland DE Jr. (1990a) Excitatory amino acid uptake and N-methyl-D-aspartate-mediated secretion in a neural cell line. Proc Natl Acad Sci U S A 87: 3518–3521. [PubMed: 1970639]

Morimoto BH and Koshland DE Jr. (1990b) Induction and expression of long- and short-term neurosecretory potentiation in a neural cell line. Neuron 5:875–880. [PubMed: 1980069]

Nakashima A, Kawamoto T, Honda KK, Ueshima T, Noshiro M, Iwata T, Fujimoto K, Kubo H, Honma S, Yorioka N, et al. (2008) DEC1 modulates the circadian phase of clock gene expression. Mol Cell Biol 28: 4080–4092. [PubMed: 18411297]

Nogales-Cadenas R, Carmona-Saez P, Vazquez M, Vicente C, Yang X, Tirado F, Carazo JM, and Pascual-Montano A (2009) GeneCodis: interpreting gene lists through enrichment analysis

and integration of diverse biological information. Nucleic Acids Res 37:W317–322. [PubMed: 19465387]

Pearson R, Fleetwood J, Eaton S, Crossley M, and Bao S (2008) Kruppel-like transcription factors: a functional family. Int J Biochem Cell Biol 40:1996–2001. [PubMed: 17904406]

Pezuk P, Mohawk JA, Wang LA, and Menaker M (2012) Glucocorticoids as entraining signals for peripheral circadian oscillators. Endocrinology 153:4775–4783. [PubMed: 22893723]

Philipsen S and Suske G (1999) A tale of three fingers: the family of mammalian Sp/XKLF transcription factors. Nucleic Acids Res 27:2991–3000. [PubMed: 10454592]

Preitner N, Damiola F, Luis Lopez M, Zakany J, Duboule D, Albrecht U, and Schibler U (2002) The orphan nuclear receptor REV-ERBα controls circadian transcription within the positive limb of the mammalian circadian oscillator. Cell 110:251–260. [PubMed: 12150932]

Raney BJ, Dreszer TR, Barber GP, Clawson H, Fujita PA, Wang T, Nguyen N, Paten B, Zweig AS, Karolchik D, et al. (2014) Track data hubs enable visualization of user-defined genome-wide annotations on the UCSC Genome Browser. Bioinformatics 30:1003–1005. [PubMed: 24227676]

Reddy TE, Gertz J, Crawford GE, Garabedian MJ, and Myers RM (2012) The hypersensitive glucocorticoid response specifically regulates period 1 and expression of circadian genes. Mol Cell Biol 32:3756–3767. [PubMed: 22801371]

Ripperger JA and Schibler U (2006) Rhythmic CLOCK-BMAL1 binding to multiple E-box motifs drives circadian Dbp transcription and chromatin transitions. Nat Genet 38:369–374. [PubMed: 16474407]

Ripperger JA, Shearman LP, Reppert SM, and Schibler U (2000) CLOCK, an essential pacemaker component, controls expression of the circadian transcription factor DBP. Genes Dev 14:679–689. [PubMed: 10733528]

Sagara Y, Dargusch R, Chambers D, Davis J, Schubert D, and Maher P (1998) Cellular mechanisms of resistance to chronic oxidative stress. Free Radic Biol Med 24:1375–1389. [PubMed: 9641255]

Sato TK, Panda S, Miraglia LJ, Reyes TM, Rudic RD, McNamara P, Naik KA, FitzGerald GA, Kay SA, and Hogenesch JB (2004) A functional genomics strategy reveals Rora as a component of the mammalian circadian clock. Neuron 43:527–537. [PubMed: 15312651]

Schibler U, Gotic I, Saini C, Gos P, Curie T, Emmenegger Y, Sinturel F, Gosselin P, Gerber A, Fluery-Olela F, et al. (2015) Clock-talk: Interactions between central and peripheral circadian oscillators in mammals. In: Grodzicker T, Steward D, and Stillman B, editors. 21st Century Genetics Genes at Work. Cold Spring Harbor (NY): Cold Spring Harbor Laboratory Press. p. 223–232,.

Sporl F, Korge S, Jurchott K, Wunderskirchner M, Schellenberg K, Heins S, Specht A, Stoll C, Klemz R, Maier B, et al. (2012) Kruppel-like factor 9 is a circadian transcription factor in human epidermis that controls proliferation of keratinocytes. Proc Natl Acad Sci U S A 109:10903–10908.

Stephan FK and Zucker I (1972) Circadian rhythms in drinking behavior and locomotor activity of rats are eliminated by hypothalamic lesions. Proc Natl Acad Sci U S A 69:1583–1586. [PubMed: 4556464]

Stratmann M, Suter DM, Molina N, Naef F, and Schibler U (2012) Circadian Dbp transcription relies on highly dynamic BMAL1-CLOCK interaction with E boxes and requires the proteasome. Mol Cell 48:277–287. [PubMed: 22981862]

Tabas-Madrid D, Nogales-Cadenas R, and Pascual-Montano A (2012) GeneCodis3: a non-redundant and modular enrichment analysis tool for functional genomics. Nucleic Acids Res 40:W478–483. [PubMed: 22573175]

Ueda HR, Chen W, Adachi A, Wakamatsu H, Hayashi S, Takasugi T, Nagano M, Nakahama K, Suzuki Y, Sugano S, et al. (2002) A transcription factor response element for gene expression during circadian night. Nature 418:534–539. [PubMed: 12152080]

Vielhaber E, Eide E, Rivers A, Gao Z-H, and Virshup DM (2000) Nuclear entry of the circadian regulator mPER1 is controlled by mammalian casein kinase I ε. Mol Cell Biol 20:4888–4899. [PubMed: 10848614]

Woodruff ER, Chun LE, Hinds LR, and Spencer RL (2016) Diurnal corticosterone presence and phase modulate clock gene expression in the male rat prefrontal cortex. Endocrinology 157:1522–1534. [PubMed: 26901093]

Yamamoto T, Nakahata Y, Tanaka M, Yoshida M, Soma H, Shinohara K, Yasuda A, Mamine T, and Takumi T (2005) Acute physical stress elevates mouse period1 mRNA expression in mouse peripheral tissues via a glucocorticoid-responsive element. J Biol Chem 280: 42036–42043. [PubMed: 16249183]

Yao M, Schulkin J, and Denver RJ (2008) Evolutionarily conserved glucocorticoid regulation of corticotropin-releasing factor expression. Endocrinology 149: 2352–2360. [PubMed: 18202128]

Yoshitane H, Ozaki H, Terajima H, Du NH, Suzuki Y, Fujimori T, Kosaka N, Shimba S, Sugano S, and Takagi T (2014) CLOCK-controlled polyphonic regulation of circadian rhythms through canonical and noncanonical E-boxes. Mol Cell Biol 34.

Zhang JS, Moncrieffe MC, Kaczynski J, Ellenrieder V, Prendergast FG, and Urrutia R (2001) A conserved alpha-helical motif mediates the interaction of Sp1-like transcriptional repressors with the corepressor mSin3A. Mol Cell Biol 21:5041–5049. [PubMed: 11438660]

Zucker SN, Fink EE, Bagati A, Mannava S, Bianchi-Smiraglia A, Bogner PN, Wawrzyniak JA, Foley C, Leonova KI, and Grimm MJ (2014) Nrf2 amplifies oxidative stress via induction of Klf9. Mol Cell 53:916–928. [PubMed: 24613345]

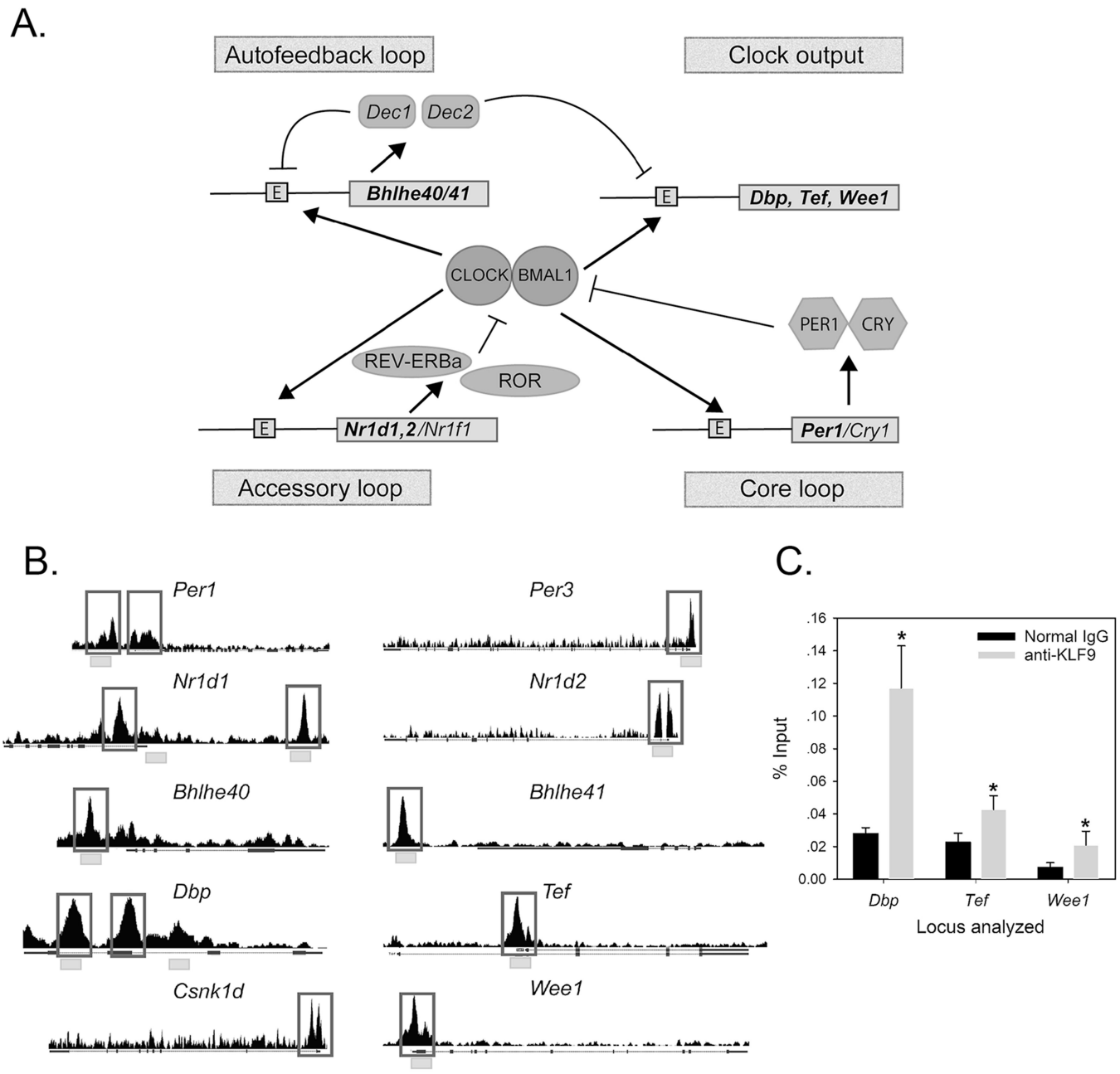

Figure 1.

Circadian clock and clock-output genes are genomic targets of KLF9 in ht22 cells and in mouse hippocampus. (a) the mammalian circadian clock consists of multiple, interacting transcription-translation feedback loops. the CLOCK and BMaL1 proteins act as transcriptional activators by binding to e-boxes as a heterodimer. among their genomic targets are *Per1/Cry1*, *Bhlhe40/41*, and *Nr1d1/Nr1f1*, whose gene products disrupt either the CLOCK+BMaL1 heterodimer or the binding of CLOCK+BMaL1 to e-boxes, thereby repressing transcription. this results in circadian variation in transcription of clock-output genes such as *Dbp*, *Tef*, and *Wee1*. Genes in bold are genomic targets of KLF9 in ht22 cells (see panel B). (B) Genome browser tracks (University of California, santa

Cruz) showing the location of KLF9 peaks at clock- and clock-output genes identified by chromatin-streptavidin precipitation followed by deep sequencing. Black boxes below the tracks indicate exons, with the direction of transcription 5′→3′, left to right. Gray boxes indicate locations of CLOCK ChiP-seq peaks identified in mouse liver by Yoshitane and colleagues (2014). C) KLF9 associates in chromatin from mouse hippocampus at *Dbp*, *Tef*, and *Wee1* genes, analyzed by chromatin immunoprecipitation assay. animals were housed on a 12:12 light:dark cycle and were sacrificed between Zt6 and Zt8. asterisks indicate statistically significant differences between antiserum to KLF9 and normal immunoglobulin G analyzed by unpaired student's *t* test ($p < 0.05$)

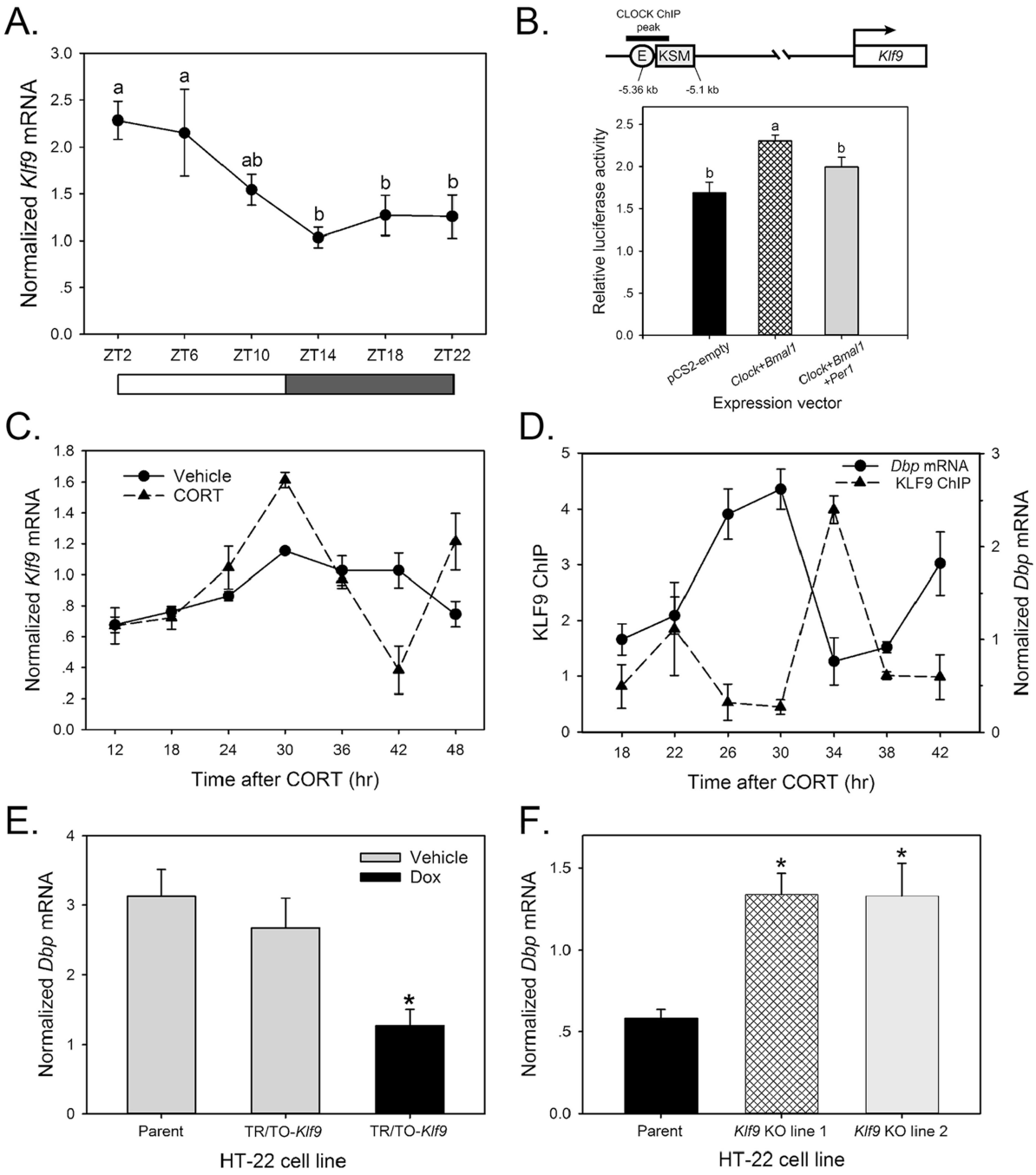

Figure 2.

Klf9 is a clock-output gene whose mRna and protein association in chromatin exhibit circadian rhythmicity. (a) Changes in *Klf9* mRna in mouse hippocampus analyzed by real-time quantitative polymerase chain reaction (Rt-qPCR) at 4-h intervals over a 20-h period. shown are the means ± seM ($n = 4$); means with the same letter are not significantly different ($p < 0.05$; analysis of variance [anOVa] followed by Fisher's least significant difference [LsD] test). animals were housed on a 12:12 light:dark cycle. Zt = zeitgeber time. Open bar indicates lights-on, and dark bar indicates lights-off. (B) the *Klf9* upstream

region contains hormone and CLOCK+BMaL1 (e-box) response elements and supports transcriptional activation by CLOCK+BMaL1. heK293 cells were co-transfected with empty vector or pshuttle-*Clock* plus pshuttle-*Bmal1* with or without pshuttle-*Per1* and 24 h later harvested and analyzed by dual luciferase assay. shown are the means ± seM ($n = 6$; $F_{2,15} = 9.858$, $p < 0.005$ anOVa); means with the same letter are not significantly different ($p < 0.05$; Fisher's LsD test). shown above the graph is a schematic depicting the *Klf9* flanking region. KsM refers to the *Klf9* synergy module (Bagamasbad et al., 2015). Gray boxes indicate the location of CLOCK ChiP-seq peaks in mouse liver (Yoshitane et al., 2014). e indicates the conserved e-box motif. numbers indicate the distance upstream of the transcription start site; its location and direction of transcription is indicated by the arrow. (C) Circadian rhythmicity in *Klf9* mRna in ht22 cells synchronized by exposure to corticosterone (CORt). Cells were plated at equal densities, treated with 1 μM CORt for 1 h to synchronize circadian gene expression at 6-h intervals through 42 h, and then all cells were harvested together at 48 h for analysis of *Klf9* mRna by Rt-qPCR. shown are the means ± seM ($n =$ 3/time point; the experiment was repeated with similar results). Circadian rhythmicity was determined using CircWave (CORt: $p < 0.05$, period = 26 h; vehicle: $p = 0.42$, no period detected). (D) Circadian rhythmicity in *Dbp* mRna and KLF9 recruitment in chromatin at the *Dbp* locus in synchronized ht22 cells. We synchronized cells with CORt at 4-h intervals up to 38 h, then harvested all cells at 42 h for analysis of *Dbp* mRna by Rt-qPCR and KLF9 recruitment to the *Dbp* locus by ChiP assay. shown are the means ± seM ($n = 3$–4/time point; the experiment was repeated with similar results). the KLF9 ChiP data are expressed as % input of anti-KLF9 serum/% input of normal rabbit serum. anOVa: *Dbp* mRna level: $F_{6,19} = 9.240$, $p < 0.001$; KLF9 ChiP data: $F_{6,16} = 6.348$, $p < 0.001$. (e) Forced expression of *Klf9* in ht22[tR/tO-*Klf9*] cells reduced *Dbp* mRna. Cells were treated with vehicle or doxycycline (Dox; 1 μg/mL) for 6 h before harvest. treatment with Dox alone did not affect the *Dbp* mRna level in the parent cell line (Knoedler et al., 2017). shown are the means ± seM ($n =$ 4/treatment; the experiment was repeated with similar results). *significantly different from the parent line by one-way anOVa ($F_{2,6} = 7.415$, $p < 0.05$) followed by holm-sidak post hoc test ($p < 0.05$). (F) elevation of the *Dbp* mRna level in *Klf9*-deficient ht22 cells. the *Klf9* gene was inactivated in ht22 cells by CRisPR/Cas9 genome editing (Knoedler et al., 2017). two independent knockout cell lines were evaluated. shown are the means ± seM ($n =$ 4/treatment; the experiment was repeated with similar results). *significantly different from the parent cell line by 1-way anOVa ($F_{2,11} = 9.441$, $p < 0.01$) followed by holm-sidak post hoc test ($p < 0.05$).

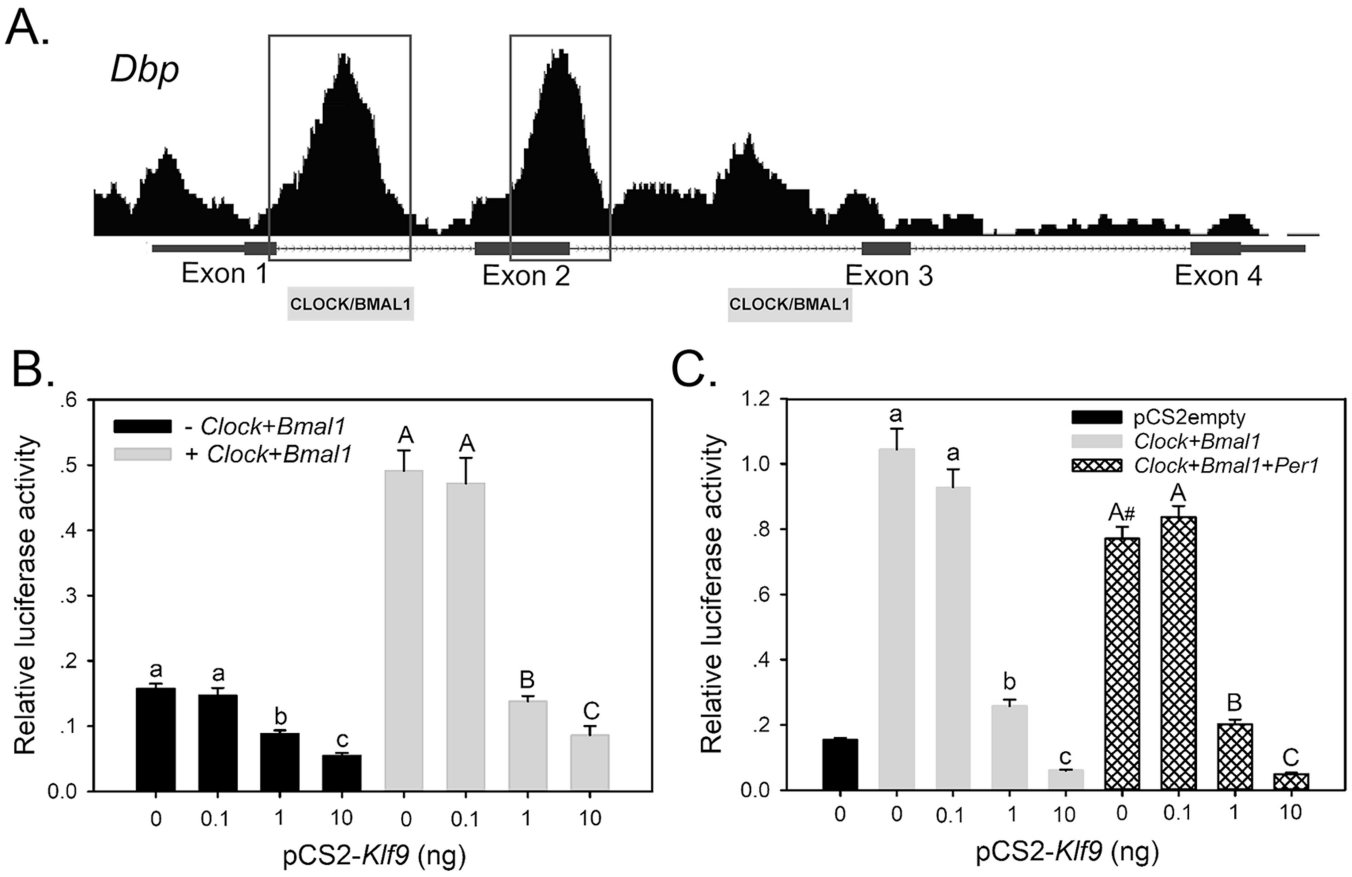

Figure 3.

Forced expression of *Klf9* strongly inhibits CLOCK+BMaL1 transcriptional activation of a *Dbp* reporter in ht22 cells. (a) KLF9 associates in chromatin at 2 sites within the mouse *Dbp* locus. shown is a genome browser track with peaks from a KLF9 chromatin-streptavidin precipitation-sequencing experiment conducted in ht22 cells (Knoedler et al., 2017). Gray boxes below the genome browser track show regions of circadian CLOCK association in chromatin identified previously by ChiP-seq (Yoshitane et al., 2014). the region in the first *Dbp* intron (left gray box) is necessary and sufficient for circadian regulation by CLOCK+BMaL1 (Ripperger et al., 2000). (B) Forced expression of *Klf9* represses baseline and CLOCK+BMaL1-dependent activation of the full-length *Dbp* reporter. We co-transfected heK293 cells with the psFV-*Dbp*-luc reporter vector with or without varying amounts of the pCs2-*Klf9* expression vector and with or without pshuttle-*Clock* plus pshuttle-*Bmal1*. We analyzed reporter activity by dual luciferase assay. Bars represent the mean ± seM ($n = 6$ wells/treatment; –*Clock*+*Bmal1:* $F_{3,20} = 56.035$, $p < 0.0001$; +*Clock*+*Bmal1:* $F_{3,19} = 75.359$, $p < 0.0001$; one-way anOVa; the experiment was repeated twice with similar results). Means with the same letter are not significantly different ($p < 0.05$, Fisher's least significant difference [LsD] post hoc test). Co-transfection of *Clock* and *Bmal1* expression vectors activated transcription by the reporter in the absence of pCs2-*Klf9* (0 dose control; $p < 0.0001$, unpaired student's *t* test). (C) Forced expression of *Per1* repressed CLOCK+BMaL1-dependent activation of the full-length *Dbp* reporter but did not affect KLF9-dependent repression. We co-transfected heK293 cells with psFV-*Dbp*-luc

with or without varying amounts of pCs2-*Klf9* and with or without pshuttle-*Clock* plus pshuttle-*Bmal1* and pshuttle-*Per1*. We analyzed reporter activity by dual luciferase assay. Bars represent the mean ± seM (n = 6 wells/treatment, *Clock*+*Bmal1:* $F_{3,20}$ = 519.512, p < 0.0001; *Clock*+*Bmal1*+*Per1:* $F_{3,20}$ = 508.002, p < 0.0001; one-way anOVa; the experiment was repeated twice with similar results). Means with the same letter are not significantly different (p < 0.05, Fisher's LsD post hoc test). [#]Co-transfection of *Per1* with *Clock*+ *Bmal1* expression vectors repressed CLOCK+BMaL1-activated transcription by the reporter in the absence of pCs2-*Klf9* (0 dose control; p = 0.002, unpaired student's t test).

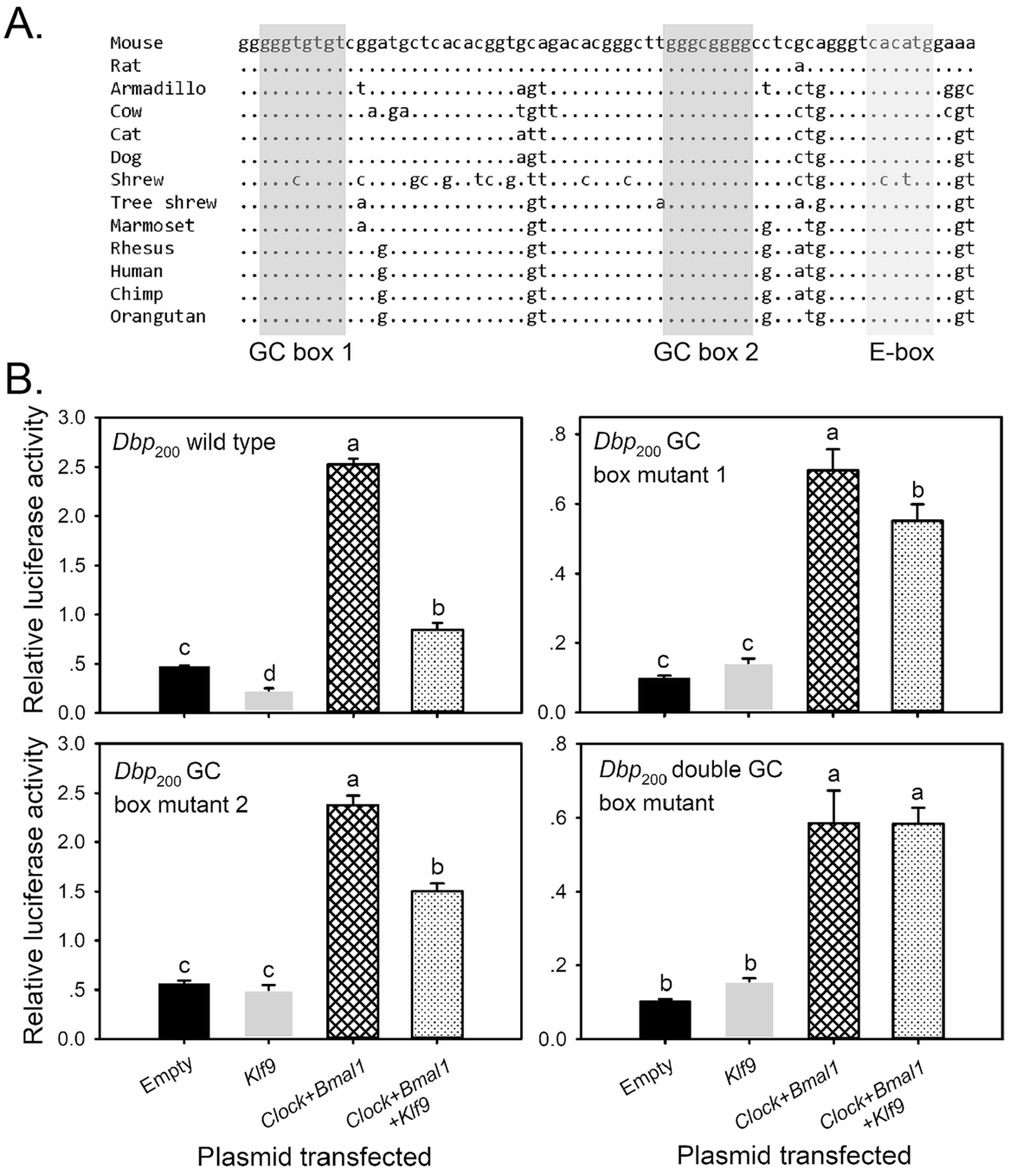

Figure 4.

Two putative KLF9 binding sites (GC boxes) found within the first *Dbp* intron are required for KLF9 repression of baseline and CLOCK+BMaL1 activation of *Dbp*. (a) the first *Dbp* intron (KLF9 ChsP-seq peak shown in Fig. 4a) contains 2 evolutionarily conserved consensus KLF9 binding motifs (GC boxes 1 and 2) located near an evolutionarily conserved e-box that was previously shown to be required for circadian changes in *Dbp* transcription (Ripperger et al., 2000). (B) Both GC boxes found within the first *Dbp* intron are required for KLF9 repression of transcription supported by a 200-bp *Dbp* reporter.

We subcloned a 200-bp fragment of the mouse *Dbp* intron containing both GC boxes and the e-box into pGL4.23 (pGL4.23-Dbp_{200}), and we conducted site-directed mutagenesis of the GC boxes. Bars represent the mean ± seM, and means with the same letter are not significantly different ($p < 0.05$, holm-sidak post hoc test). experiments were repeated twice with similar results. Upper left: Forced expression of *Klf9* repressed baseline and CLOCK+BMaL1-dependent activation of pGL4.23-Dbp_{200}. We co-transfected heK293 cells with the pGL4.23-Dbp_{200} reporter vector with or without varying amounts of the pCs2-*Klf9* expression vector and with or without pshuttle-*Clock* plus pshuttle-*Bmal1*. We analyzed reporter activity by dual luciferase assay ($n = 4$ wells/treatment, $F_{3,15} = 475.473$, $p < 0.001$, one-way anOVa; the experiment was repeated twice with similar results). Upper right: Mutation of GC box 1 eliminated KLF9 repression of baseline transcription and reduced KLF9 repression of CLOCK+BMaL1-dependent activation ($n = 4$ wells/treatment $F_{3,15} = 58.057$, $p < 0.001$). Lower left: Mutation of GC box 2 eliminated KLF9 repression of baseline transcription and reduced KLF9-repression of CLOCK+BMaL1-dependent activation ($F_{3,15} = 167.966$, $p < 0.001$). Lower right: Mutation of both GC boxes eliminated KLF9 repression of baseline transcription and also KLF9 repression of CLOCK+BMaL1-dependent activation ($n = 4$ wells/treatment, $F_{3,15} = 28.394$, $p < 0.001$).

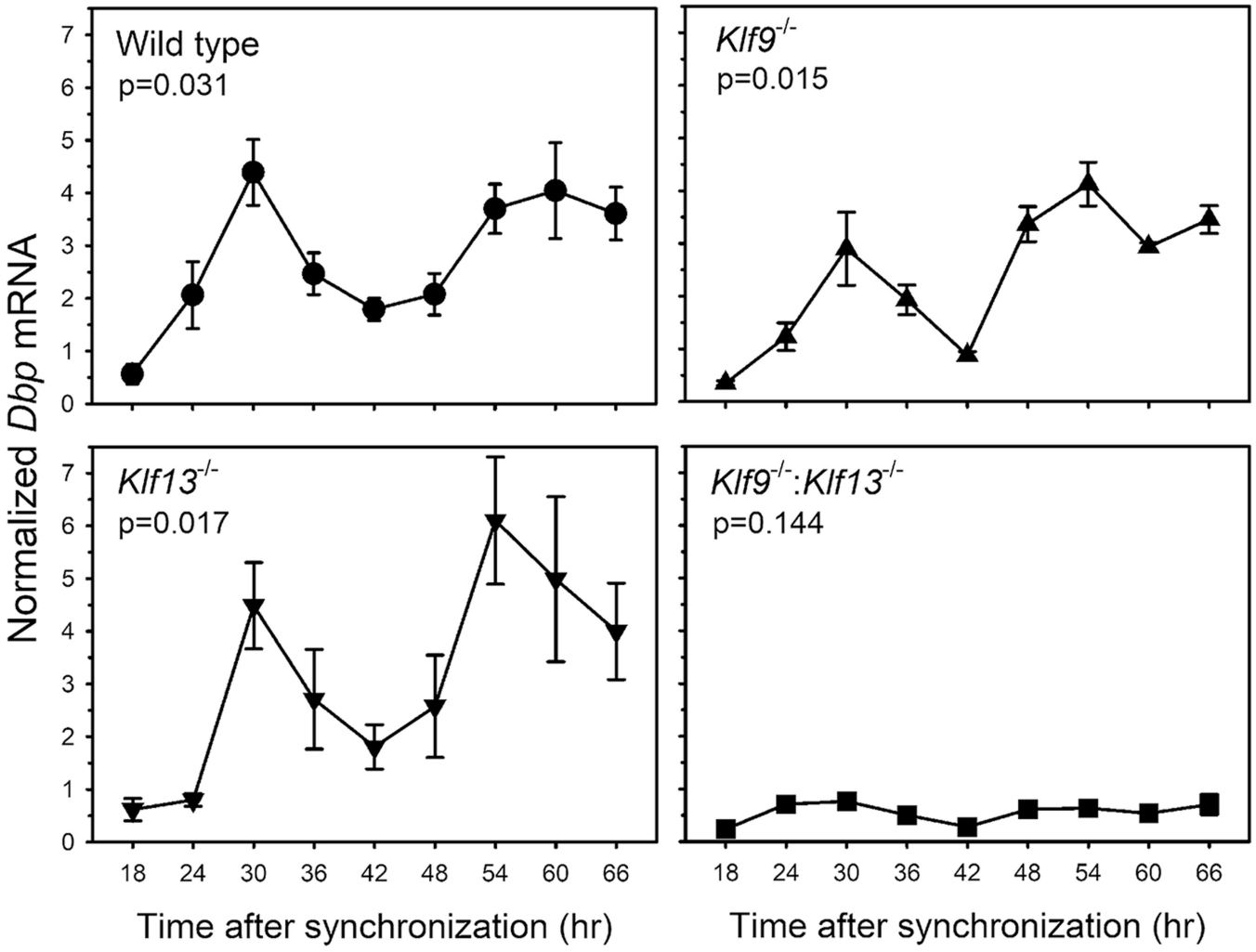

Figure 5.

Circadian rhythmicity in *Dbp* mRna was abolished in *Klf9* and *Klf13* double knockout ht22 cells. We created single and double knockout cells using CRisPR/Cas9 genome editing. We plated cells at equal densities, treated with 1 μM CORt for 1 h at 6-h intervals through 60 h to synchronize circadian gene expression, and then all cells were harvested together at 66 h for analysis of *Dbp* mRna by real-time quantitative polymerase chain reaction. We analyzed circadian rhythmicity using CircWave software. the ht22 parent cell line (wild type) showed statistically significant circadian oscillation in *Dbp* mRna. Mutation of *Klf9* or *Klf13* alone did not affect the *Dbp* mRna rhythm. By contrast, regular oscillations in *Dbp* mRna were abolished in the double knockout cells. each point represents the mean ± seM (n = 4/treatment).

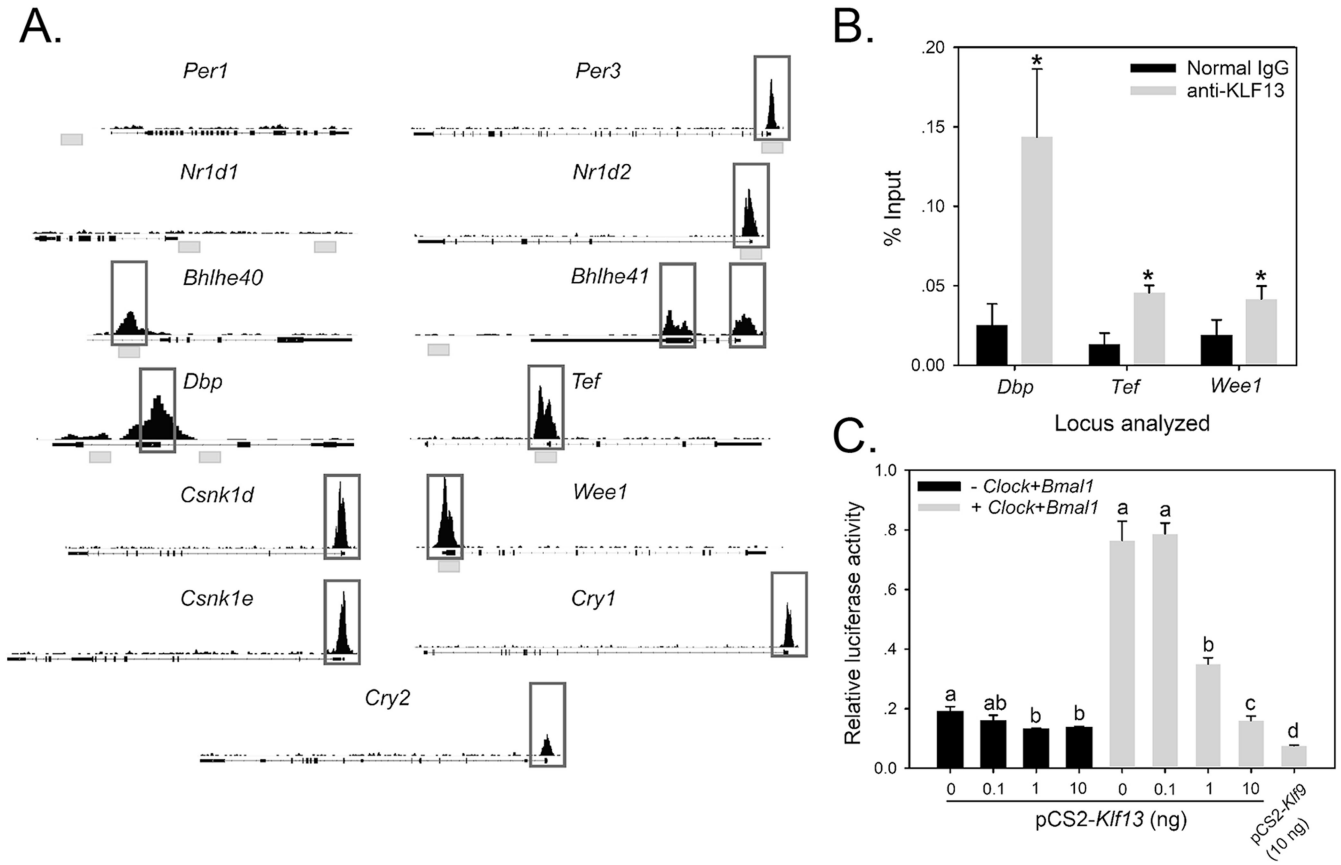

Figure 6.

Circadian clock and clock-output genes are genomic targets of KLF13 in ht22 cells and in mouse hippocampus; KLF13 may regulate multiple components of the cellular circadian clock. (a) Genome browser tracks (University of California, santa Cruz) showing the location of KLF13 peaks at clock and clock-output genes identified by chromatin-streptavidin precipitation followed by deep sequencing in ht22 cells. Black boxes below the tracks indicate exons, with the direction of transcription 5′→3′, left to right. Gray boxes indicate locations of CLOCK ChiP-seq peaks identified in mouse liver by Yoshitane and colleagues (2014). (B) KLF13 associates in chromatin from mouse hippocampus at *Dbp, Tef*, and *Wee1* genes, analyzed by chromatin immunoprecipitation assay. asterisks indicate statistically significant differences between antiserum to KLF13 and normal immunoglobulin G analyzed by unpaired student's *t* test ($p < 0.05$). (C) Forced expression of *Klf13* represses baseline and CLOCK+BMaL1-dependent activation of the full-length *Dbp* reporter. We co-transfected heK293 cells with the psFV-*Dbp*-luc reporter vector with or without varying amounts of the pcDna4:tO-*Klf13* expression vector and with or without pshuttle-*Clock* plus pshuttle-*Bmal1*. We analyzed reporter activity by dual luciferase assay. Bars represent the mean ± seM ($n = 4$ wells/treatment; –*Clock*+*Bmal1:* $F_{3,12} = 6.371$, $p = 0.008$; +*Clock*+*Bmal1:* $F_{3,12} = 136.637$, $p < 0.0001$; analysis of variance; the experiment was repeated twice with similar results). Means with the same letter are not significantly different ($p < 0.05$, Fisher's least significant difference post hoc test). Co-transfection of

Clock and *Bmal1* expression vectors activated transcription by the reporter in the absence of pcDna4:tO-*Klf13* (0 dose control; $p < 0.0001$, unpaired student's *t* test).